Dispersion of Bound Electronic Nonlinear Refraction in Solids

Mansoor Sheik-Bahae, *Member, IEEE*, David Crichton Hutchings, David J. Hagan, *Member, IEEE*, and Eric W. Van Stryland, *Senior Member, IEEE*

***Abstract*—A two-band model is used to calculate the scaling and spectrum of the nondegenerate nonlinear absorption $\Delta\alpha(\omega_1;\omega_2)$. From this, the bound electronic nonlinear refractive index n_2 is obtained using a Kramers–Krönig transformation. We include the effects of two-photon and Raman transitions and the ac Stark shift (virtual band blocking). The theoretical calculation for n_2 shows excellent agreement with measured values for a five order of magnitude variation in the modulus of n_2 in semiconductors and wide-gap optical solids. We also present new measurements of n_2 in semiconductors using the Z-scan method. The observed change of sign of n_2 midway between the two-photon absorption edge and the fundamental absorption edge is also predicted. Thus, we now have a comprehensive theory that allows a determination of n_2 at wavelengths beneath the band edge, given only the bandgap energy and the linear index of refraction. Such information is useful for a variety of applications including optical limiting, laser-induced damage, and all-optical switching. Some consequences for all-optical switching are discussed, and a wavelength criterion for the observation of switching is derived.**

I. Introduction

RECENTLY we reported measurements of the nonlinear refractive index n_2 of a variety of solids using beam distortion methods (Z-scan technique) [1], [2] and four-wave mixing [3]. These data show a strong systematic dispersion of the bound electronic nonlinearity (electronic Kerr effect n_2) near the two-photon absorption (2PA) edge. This eventually turns from positive to negative at higher frequencies. We found that by using a Kramers–Krönig (KK) integral based on the degenerate 2PA spectrum as predicted by a two-parabolic band model, we could predict the observed universal dispersion, scaling, and values of n_2 that range over four orders of magnitude and change sign [2]. This KK analysis relates the real and imaginary parts of the third-order susceptibility. The resulting scaling rule correctly predicted the value of n_2 for the 26 different materials we had examined at that time, except very near the gap where there was a systematic departure of the data from the theory towards larger negative n_2 values. More recent data taken at wavelengths closer to the gap show an even larger departure from the predictions of the 2PA model. We had speculated in [2] that the bandgap resonant ac Stark effect might make $|n_2|$ larger near the gap. Here, we present a model that includes the ac Stark effect and the electronic Raman effect, as well as 2PA. Indeed, the inclusion of these new effects does explain the large negative increase in n_2 near the gap.

There are two distinct frequency regimes for nonlinear optics in semiconductors which correspond to real and virtual excitation. Most studies have primarily concentrated on bandgap resonant effects which result in real excitation [4], [5]. The very large nonlinear effects observed are the saturation of interband and excitonic absorption due to photoexcited free carriers and excitons. Real excitations usually result in a reduction of the refractive index at frequencies of interest. In contrast, by exciting optical solids at frequencies much less than the gap, a considerably smaller, but faster, positive nonlinear refractive index n_2 due to bound electronic effects is observed [6]. This n_2 arises from the real part of the third-order susceptibility $\chi^{(3)}$, and is defined through the refractive index change Δn where

$$\Delta n(\omega) = \gamma(\omega) I_\omega = n_2(\omega) \frac{|E_\omega|^2}{2} \tag{1}$$

with I_ω and E_ω being the irradiance and electric field at frequency ω, respectively, and $n_2 \propto \mathrm{Re}\,\chi^{(3)}/n_0$. The linear refractive index is n_0, and γ and n_2 are related by n_2 (esu) $= cn_0\gamma/40\pi$ (SI) where c is the speed of light. The magnitude and dispersion of n_2 is of interest because of its importance in applications such as nonlinear propagation in fibers, fast optical switching, self-focusing and damage in optical materials, and optical limiting in semiconductors [7]–[9].

Measurements of wide bandgap dielectrics show that $n_2 > 0$, which explains catastrophic self-focusing damage in such materials as NaCl and SiO_2 [8]. Our measurements in semiconductors below or near the 2PA edge ($\hbar\omega \simeq E_g/2$) also show positive n_2. However, we found recently that for wavelengths substantially above the 2PA edge, n_2 is negative [1]. We performed measurements on

Manuscript received October 19, 1990; revised February 7, 1991. This work was supported by the National Science Foundation under Grant ECS 8617066, by DARPA/CNVEO, and by the Florida High Technology and Industry Council.

M. Sheik-Bahae and D. C. Hutchings are with the Center for Research in Electro-Optics and Lasers (CREOL), University of Central Florida, Orlando, FL 32826.

D. J. Hagan is with the Center for Research in Electro-Optics and Lasers (CREOL) and the Department of Physics, University of Central Florida, Orlando, FL 32826.

E. W. Van Stryland is with the Center for Research in Electro-Optics and Lasers (CREOL) and the Departments of Physics and Electrical Engineering, University of Central Florida, Orlando, FL 32826.

IEEE Log Number 9144871.

a large number of other materials, including semiconductors and dielectrics, above and below the 2PA edge. As a result, we have been able to clearly demonstrate the dispersion of n_2.

Our measurements utilized a newly developed sensitive technique (Z scan) [1], [10] that accurately determines the magnitude and sign of n_2, even in the presence of 2PA where it also gives the 2PA coefficient β. For example we found a negative n_2 in materials such as ZnSe at 0.523 μm where 2PA is present, and a positive n_2 at 1.064 μm where 2PA is absent. The values obtained for β were in excellent agreement with our earlier measurements using standard transmission experiments [11]. We also performed picosecond degenerate four-wave mixing (DFWM) measurements which showed this third-order response to be fast (time resolution limited by the 30 ps pulsewidth). At wavelengths where 2PA was present, this fast third-order nonlinearity was dominant at low irradiance (e.g., up to 0.5 GW/cm^2 in ZnSe at 532 nm), while at higher irradiance, the slowly decaying 2PA-generated free-carrier refraction (self-defocusing) became important [3]. DFWM studies in other semiconductors and other wavelengths showed this to be a universal phenomenon [12].

It has previously been predicted that $\chi^{(3)}$ should vary as E_g^{-4} [13]. Using this scaling and the relation between n_2 and $\chi^{(3)}$ that includes the linear index n_0, we can remove the E_g and n_0 dependencies from the experimental values of n_2 by multiplying them by $n_0 E_g^4$. In Fig. 1, a plot of our experimentally determined scaled values of n_2 as a function of $\hbar\omega/E_g$ is shown. We also divide the data by a constant K' which we explain in what follows. We show, on the same plot, several data for large-gap optical crystals obtained from recent measurements by Adair *et al.* using a "nearly degenerate three-wave mixing" scheme [6]. Our own measurements of several of the same materials studied in [6] show excellent absolute agreement. Assuming that there are no other relevant parameters unique to each material other than bandgap and index, this plot should be general to all optical solids. Upon examination of Fig. 1, we immediately see a trend giving small positive values for low ratios of photon energy to bandgap energy which slowly rises to a broad resonance peak at the 2PA edge and then decreases, eventually turning negative between the two-photon and single-photon absorption edges. We should note that the scaling with E_g hides a variation in magnitude of n_2 of four orders of magnitude so that the observation of a universal dispersion curve as in Fig. 1 is quite remarkable. This dispersion curve is qualitatively similar to the dispersion of the linear index around the single-photon absorption edge [14]. As these linear quantities are related by causality via a KK relation, it seems logical to investigate whether the observed dispersion of n_2 can be calculated using a nonlinear KK relation between the real and imaginary parts of $\chi^{(3)}$. Indeed, as we showed in [2], making some reasonable assumptions, the observed tendencies as well as the absolute magnitudes of this dispersion are well predicted by such a calculation. The solid line in Fig. 1 as reproduced from [2] is the direct result of such a calculation, including only the degenerate 2PA contribution to the imaginary part of $\chi^{(3)}$. It should be noted that since the 2PA spectrum was previously determined [11], [13], [15], no additional fitting parameter was used in this calculation.

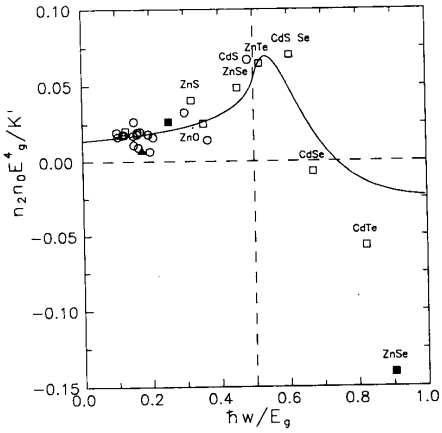

Fig. 1. Data of n_2 scaled as $n_2 n_0 E_g^4/K'$ versus $\hbar\omega/E_g$ from [2]. Note that the definition of the constant K' in this reference differs slightly from that used in this paper. These data include measurements of n_2 at 1.06 μm in [6], as well as our own measurements at 1.06 and 0.53 μm. Recent measurements have revised some of the semiconductor n_2 values shown in this figure (see Fig. 5). The solid line demonstrates the fit obtained in [2] using a quasi-degenerate 2PA.

II. Kramers–Krönig (KK) Relation

Most theoretical calculations of n_2 have been confined to the zero-frequency limit [16]–[20]. Of these, semi-empirical formulations have been the most successful in predicting the magnitude of n_2 [19], [20]. For example, the formula obtained by Boling, Glass, and Owyoung (BGO) in relating n_2 to the linear index (n_0) and the dispersion of n_0 in terms of the Abbe number has been successfully applied to a large class of transparent materials [6], [20]. Their theory predicts the low-frequency magnitude of n_2, but does not give the dispersion. The KK method predicts the dispersion as well as the magnitude of n_2. While the calculation presented in [2] only included 2PA in the imaginary part of $\chi^{(3)}$, the present calculation includes all other relevant contributions, that is, from electronic Raman and the ac Stark effect ("virtual band blocking"). We, however, do not include possible effects from excitonic enhancement [21].

Based on the principle of causality, KK relates the refractive index and the absorption coefficient for any linear material [22]:

$$n(\omega) - 1 = \frac{c}{\pi} \int_0^\infty \frac{\alpha(\omega')}{\omega'^2 - \omega^2}\, d\omega'. \tag{2}$$

We now introduce some perturbation ξ into the system, and consider the change in the refractive index resulting from the effect of ξ. The KK transformation states that a

change in the refractive index (Δn) at ω is associated with changes in the absorption coefficient ($\Delta\alpha$) throughout the spectrum (ω') and vice versa. We write this as

$$\Delta n(\omega;\ \xi) = \frac{c}{\pi}\int_0^\infty \frac{\Delta\alpha(\omega';\ \xi)}{\omega'^2 - \omega^2}\,d\omega' \tag{3}$$

where ξ is a parameter (or parameters) denoting the "cause" of change in the absorption.

The cause need not be of optical origin, but of any external perturbation. For example, this method has been used to calculate the refractive index change resulting from an excited electron–hole plasma [23] and a thermal shift of the band edge [24]. For cases where an electron–hole plasma is injected, the consequent change of absorption gives the plasma contribution to the refractive index. In this case, the ξ parameter is taken as the change in plasma density (ΔN) regardless of the mechanism of generation of the plasma or the pump frequency. In the case of 2PA, the change is due to the presence of a pump field of frequency Ω (i.e., $\xi = \Omega$). The corresponding nonlinear refraction is $\Delta n(\omega;\ \Omega)$, which gives the index change at ω due to the presence of light at Ω. Although the calculation as illustrated above gives the nondegenerate nonlinear refraction, in most cases we would set $\Omega = \omega$ and consider self-refraction. This gives what is commonly referred to as n_2. Van Vechten and Aspnes [18] obtained the low-frequency limit of n_2 from a similar KK transformation of the Franz–Keldysh electroabsorption effect where, in this case, ξ is the dc field. It is important to note that we must set $\Omega = \omega$ and not $\Omega = \omega'$, otherwise nonlinear KK relations do not apply as shown, for example, for the two-level atom [25]. The bound electronic contribution to $\chi^{(3)}$ can originate from various absorptive counterparts that are quadratic functions of the pump field. Effects of this order are 2PA, the electronic Raman effect, and the optical Stark effect.

An alternative way of considering the nonlinear Kramers–Krönig calculation is to examine the causality of the system. By treating the system as consisting of the material plus light, causality relations between the nonlinear polarization and an additional light field give rise to relations between the real and imaginary parts of $\chi^{(3)}$ [26], [27] in an analogous way to the usual "linear" Kramers–Krönig relations. These resulting relations can be reexpressed in the form given above. One can therefore think of the nonlinear KK relations as being not on a bare material, but on a system consisting of the material and an optical pump.

In order to perform the KK calculation, it is necessary to know the nondegenerate absorption $\Delta\alpha(\omega, \Omega)$, which is the absorption of light at frequency ω when a light field of frequency Ω is applied to the material. This is necessary even if only self-refraction is desired. In what follows, we calculate the nondegenerate absorption originating from $\chi^{(3)}$, including the 2PA, ac Stark, and Raman contributions. The degenerate 2PA result, found by setting $\omega = \Omega$, will serve as a check against previous theoretical and experimental results.

Although nondegenerate nonlinear absorption is required for the correct calculation of n_2, an estimate can be obtained by substituting the degenerate 2PA at the mean frequency for the nondegenerate absorption:

$$\Delta\alpha(\omega;\ \omega') \rightarrow \beta\left(\frac{\omega + \omega'}{2}\right)I_{\omega'}. \tag{4}$$

This calculation was presented in [2]. We note that (4) provides a good estimate of n_2, except close to the band edge where the ac Stark contribution becomes large. This agreement reflects the fact that the denominator in the KK integrand (3) has the effect of strongly weighting frequencies close to ω', so for self-refraction, $\Delta\alpha(\omega;\ \omega')$ needs to be known accurately only for ω in the vicinity of ω'. This approximation breaks down, however, when it is necessary to include divergent terms such as the ac Stark effect.

III. Nonlinear Absorption Calculation

Two-photon absorption processes require that perturbation theory be taken to second order. A variation of this is to use first-order perturbation theory on "dressed" states for the conduction and valence bands where the effect of the acceleration (tunneling) of the electrons due to the oscillating electric field is already taken into account [28], [29]. In all of the following, we shall use the dipole approximation for the radiation interaction Hamiltonian:

$$\mathcal{H}_{\text{int}} = -\frac{e}{m_0 c}\boldsymbol{A}\cdot\boldsymbol{p} \tag{5}$$

where $\boldsymbol{A}$ is the magnetic vector potential, $\boldsymbol{p}$ is the electron momentum operator, $-e$ is the electron charge, and m_0 is the free electron mass. We assume a two-beam interaction with both beams linearly polarized in the same direction, giving

$$\boldsymbol{A} = \hat{\boldsymbol{a}}[A_{01}\cos(\omega_1 t) + A_{02}\cos(\omega_2 t + \phi)] \tag{6}$$

where $\hat{\boldsymbol{a}}$ is the unit vector in the direction of the optical polarization. Following Keldysh [28], in the same manner as [29], [30], such a dressed state can be approximated by a Valkov-type wavefunction [31]:

$$\psi_i(\boldsymbol{k},\ \boldsymbol{r},\ t) = u_i(\boldsymbol{k},\ \boldsymbol{r})\exp\left[i\boldsymbol{k}\cdot\boldsymbol{r} - \frac{i}{\hbar}\int_0^t E_i(\tau)\,d\tau\right] \tag{7}$$

where i refers to either the conduction or valence band. $u_i(\boldsymbol{k},\ \boldsymbol{r})$ are the usual Bloch wavefunctions which have the same periodicity as the lattice. The effect of the optical field is to alter the energy of the electrons and holes in the final and initial states, respectively. Only the first- and second-order ac Stark shifting of the bands give rise to a $\chi^{(3)}$ effect:

$$E_c(\tau) = E_{c0} + \Delta E_{cc}(\tau) + \Delta E_{cv} \tag{8}$$

$$E_v(\tau) = E_{v0} + \Delta E_{vv}(\tau) + \Delta E_{vc} \tag{9}$$

where, within the effective mass approximation,

$$E_{c0} = E_g + \frac{\hbar^2 k^2}{2m_c c} \tag{10}$$

$$E_{v0} = \frac{\hbar^2 k^2}{2m_v c} \tag{11}$$

$$\Delta E_{ii}(\tau) = \frac{-e\hbar}{m_i c} \boldsymbol{k} \cdot \boldsymbol{A}(\tau) \tag{12}$$

where we have defined the hole mass m_v as being negative. ΔE_{cv} and ΔE_{vc} are the time-independent quadratic ac Stark shifts of the bands, which are proportional to $|A_0|^2$ and will be discussed in Section III-C. The transition rates will be calculated using an S-matrix formalism [32], with

$$S = -\frac{i}{\hbar} \int_{-\infty}^{\infty} dt \int d^3 r\, \psi_c^*(\boldsymbol{k}, \boldsymbol{r}, t) \mathcal{H}_{\text{int}} \psi_v(\boldsymbol{k}', \boldsymbol{r}, t). \tag{13}$$

The resulting S matrix for these processes is

$$S = \frac{i}{\hbar} \frac{e\hat{\boldsymbol{a}} \cdot \boldsymbol{p}_{vc}}{m_0 c} \delta_{kk'} \int_{-\infty}^{\infty} dt \cdot e^{i\omega_{vc} t} [A_{01} \cos(\omega_1 t) + A_{02} \cos(\omega_2 t + \phi)] \cdot \exp[i\eta_1 \sin(\omega_1 t) + i\eta_2 \sin(\omega_2 t + \phi)] \tag{14}$$

where $\boldsymbol{p}_{vc}$ is the interband momentum matrix element given by

$$\boldsymbol{p}_{vc} = \frac{i}{\hbar} \int d^3 r\, u_c^*(\boldsymbol{k}, \boldsymbol{r}) \nabla u_v(\boldsymbol{k}, \boldsymbol{r}). \tag{15}$$

We define

$$\hbar\omega_{vc} = E_g - \Delta E_{vc} + \Delta E_{cv} + \frac{\hbar^2 k^2}{2m_{vc}} \tag{16}$$

the reduced mass, by

$$\frac{1}{m_{vc}} = \frac{1}{m_c} - \frac{1}{m_v} \tag{17}$$

and

$$\eta_j = \frac{eA_{0j} \boldsymbol{k} \cdot \hat{\boldsymbol{a}}}{m_{vc} c \omega_j}. \tag{18}$$

In order to perform the time integral, we make use of the identity

$$\exp[i\eta \sin(\omega t)] = \sum_{n=-\infty}^{\infty} J_n(\eta) e^{in\omega t}. \tag{19}$$

On substitution and performing the time integral, the S matrix becomes

$$S = \frac{i\pi}{\hbar} \frac{e\hat{\boldsymbol{a}} \cdot \boldsymbol{p}_{vc}}{m_0 c} \sum_{m,n=-\infty}^{\infty} J_m(\eta_1) J_n(\eta_2) \cdot \{A_{01}[\delta((m+1)\omega_1 + n\omega_2 + \omega_{vc}) + \delta((m-1)\omega_1 + n\omega_2 + \omega_{vc})] + A_{02}[\delta(m\omega_1 + (n+1)\omega_2 + \omega_{vc}) + \delta(m\omega_1 + (n-1)\omega_2 + \omega_{vc})]\}. \tag{20}$$

A. Degenerate 2PA Calculation

The delta function terms in the above expression indicate various combinations of multiphoton absorption processes. From the S-matrix description, transition rates can be determined [32] which lead to absorption coefficients. We first consider 2PA at frequency ω_1 in order to determine the scaling. Therefore, consider the terms arising from $A_{02} = 0$, $m = -1$, $n = 0$. Using the lowest order MacLaurin expansion term for the Bessel function $J_n(x) \simeq x^n/2^n n!$, and ignoring the quadratic Stark shift terms for now, the resulting change in the transition rate due to 2PA is

$$\Delta W = \sum_{\text{spin}} \int \frac{d^3 k}{(2\pi)^3} \left[\frac{\pi e^2 A_{01}^2}{2m_0 m_{vc} c^2 \omega_1}\right]^2 |\hat{\boldsymbol{a}} \cdot \boldsymbol{p}_{vc}|^2 \cdot |\boldsymbol{k} \cdot \hat{\boldsymbol{a}}|^2 \frac{1}{2\pi\hbar} \delta\left(E_g + \frac{\hbar^2 k^2}{2m_{vc}} - 2\hbar\omega_1\right). \tag{21}$$

A two-band model will be used in this paper for the calculation of transition rates, consisting of a conduction band and a valence band of opposite curvature ($m_v = -m_c$), each of which is doubly degenerate in spin. We will consider parabolic bands only. There is an angular dependence in k space for the $|\hat{\boldsymbol{a}} \cdot \boldsymbol{p}_{vc}|^2$ and $|\boldsymbol{k} \cdot \hat{\boldsymbol{a}}|^2$ terms, which results in a factor of $1/5$ when the angular integral is performed, assuming that $\boldsymbol{p}_{vc}$ is parallel to $\boldsymbol{k}$. For other cases, the resulting transition rate will have the same functional form and only differ by a numeric factor. For instance, in the Kane four-band model for the heavy-hole band, $\boldsymbol{p}_{vc}$ is perpendicular to $\boldsymbol{k}$ [33] and the numeric factor is $2/15$.

Using the fact that $A_{0j}^2 = 8\pi c I_j / n_j \omega_j^2$ where I_j is the irradiance (cgs) and n_j is the linear index, the result for the change in transition rate is

$$\Delta W = \frac{2^4 \pi}{5} \frac{e^4}{n_1^2 c^2} \frac{m_c^{1/2} |\boldsymbol{p}_{vc}|^2}{m_0^2} \frac{I_1^2}{(\hbar\omega_1)^6} (2\hbar\omega_1 - E_g)^{3/2} \tag{22}$$

from which the two-photon absorption rate can be determined; $\beta(\omega) = 2\hbar\omega\, \Delta W I_1^{-2}$. In order to obtain a universal scaling law, we make use of the identity

$$\frac{|\boldsymbol{p}_{vc}|^2}{m_0^2} \simeq \frac{E_g}{2m_c}, \tag{23}$$

which is obtained using $\boldsymbol{k} \cdot \boldsymbol{p}$ theory [33]. The resulting expression for the 2PA has exactly the same scaling and frequency dependence as that calculated in [13], [15] using the second-order perturbation approach, namely,

$$\beta(\omega) = K \frac{\sqrt{E_p}}{n_0^2 E_g^3} F_2\left(\frac{\hbar\omega}{E_g}\right) \tag{24}$$

where $E_p = 2|\boldsymbol{p}_{vc}|^2/m_0$ and

$$F_2(x) = \frac{(2x-1)^{3/2}}{(2x)^5}. \tag{25}$$

Note that $\beta \propto \omega \operatorname{Im} \chi^{(3)}/n_0$. The function F_2 is only a function of the ratio of the photon energy $\hbar\omega$ to E_g (i.e., denoting the optically coupled states). The functional form of F_2 reflects the assumed band structure and the intermediate states considered in calculating the 2PA transition rate. E_p is nearly material independent and possesses a value $E_p \simeq 21$ eV for most direct gap semiconductors, and K is a material-independent constant:

$$K = \frac{2^9\pi}{5} \frac{e^4}{\sqrt{m_0 c^2}} \tag{26}$$

which has a value of $K = 1940$ in units such that β is in cm/GW and E_g and E_p are in eV. A wealth of experimental and theoretical work regarding 2PA in semiconductors and crystalline materials exists. The best fit to the data of [11] using (24) and (25) gave $K = 3100$ in the same units as above, while Weiler's second-order perturbation calculation for a four-band model gave $K = 5200$ for parabolic bands neglecting any coulomb interaction [15]. When nonparabolicity was included, the predicted values of β were on average only 26% higher than experiment; however, the frequency dependence of β changed very little. Interestingly, (24) and (25) also give a fair estimate of β for a number of transparent materials measured using the third and fourth harmonics of picosecond Nd:YAG laser pulses [34], [9]. In Fig. 2, β scaled by $n_0^2/(K\sqrt{E_p}F_2)$ versus E_g on a log-log plot is shown. The slope of the straight line is -3, and it shows good agreement with the data for semiconductors and is within a factor of $\simeq 5$, even for wide-gap dielectrics [9].

B. Nondegenerate 2PA and Raman Transitions

We now consider the case where one photon from each of (ω_1, ω_2) is absorbed, i.e., terms which contain $\delta(\omega_{vc} - \omega_1 - \omega_2)$, $\delta(\omega_{vc} - \omega_1 + \omega_2)$, and $\delta(\omega_{vc} + \omega_1 - \omega_2)$ in (20). The first term corresponds to nondegenerate 2PA, whereas the second and third terms correspond to Raman transitions. On performing the integral over k space, it can be shown that for 2PA, the change in the transition

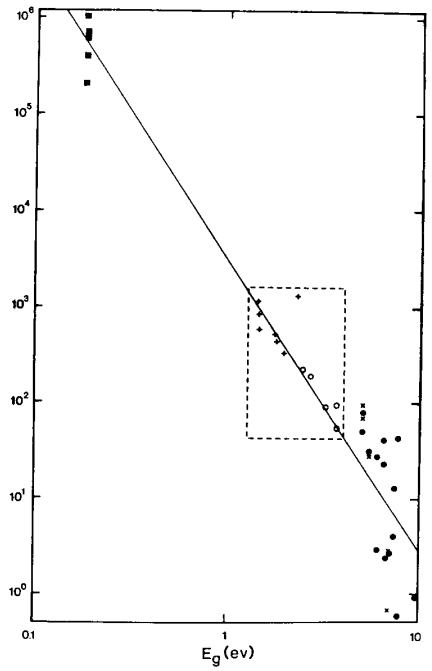

Fig. 2. A log-log plot of the scaled two-photon absorption coefficient $\beta n_0^2/K\sqrt{E_p}F_2$ versus energy gap from [9]. The solid line is a least squares fit of the semiconductor data enclosed by the dashed box to a line of slope -3. The fit also gives a good estimate of 2PA in wide-gap optical solids (lower right) [34] and InSb (upper left) [35].

rate is given as

$$\begin{aligned}\Delta W = \sum_{\text{spin}} \int \frac{d^3k}{(2\pi)^3} \left[\frac{\pi e^2 A_{01} A_{02}}{2m_0 m_{vc} c^2}\right]^2 |\hat{\boldsymbol{a}} \cdot \boldsymbol{p}_{vc}|^2 |\boldsymbol{k} \cdot \hat{\boldsymbol{a}}|^2 \\ \cdot \left(\frac{1}{\omega_1} + \frac{1}{\omega_2}\right)^2 \frac{1}{2\pi\hbar} \delta\left(E_g + \frac{\hbar^2 k^2}{2m_{vc}} - \hbar\omega_1 - \hbar\omega_2\right) \\ = \frac{2^4\pi}{5} \frac{e^4}{n_1 n_2 c^2} \frac{m_c^{1/2} |\boldsymbol{p}_{vc}|^2}{m_0^2} \frac{I_1 I_2}{(\hbar\omega_1)^2 (\hbar\omega_2)^2} \\ \cdot \left(\frac{1}{\hbar\omega_1} + \frac{1}{\hbar\omega_2}\right)^2 (\hbar\omega_1 + \hbar\omega_2 - E_g)^{3/2}.\end{aligned} \tag{27}$$

Using this expression for the transition rate, a change in absorption of the ω_1 beam due to the presence of ω_2 is calculated to have the general form

$$\Delta\alpha(\omega_1; \omega_2) = 2K \frac{\sqrt{E_p}}{n_1 n_2 E_g^3} F_2\left(\frac{\hbar\omega_1}{E_g}; \frac{\hbar\omega_2}{E_g}\right) I_2 \tag{28}$$

where for nondegenerate 2PA, the F_2 function as obtained from (27) is given by

$$F_2^{\text{2PA}}(x_1; x_2) = \frac{(x_1 + x_2 - 1)^{3/2}}{2^7 x_1 x_2^2} \left(\frac{1}{x_1} + \frac{1}{x_2}\right)^2. \tag{29}$$

Needless to say, F_2^{2PA}, and hence 2PA, is zero when $(x_1 + x_2 - 1) < 0$.

In a similar manner, the Raman terms can be calculated to give a change in absorption as in (28) with

$$F_2^{\mathrm{RAM}}(x_1; x_2) = \frac{(x_1 - x_2 - 1)^{3/2} - (-x_1 + x_2 - 1)^{3/2}}{2^7 x_1 x_2^2} \cdot \left(\frac{1}{x_1} - \frac{1}{x_2}\right)^2. \tag{30}$$

The above expression contains the Raman transitions in which an electron is excited from the valence band into the conduction band via absorption of a photon at $\hbar\omega_1$ and emission of a photon at $\hbar\omega_2$ and vice versa. Therefore, the energy conservation terms corresponding to these transitions denoted by the $(\cdots)^{3/2}$ terms in (30) are zero when their argument is negative.

The total $\Delta\alpha(\omega_1; \omega_2)$ from these multiphoton processes is the sum of the 2PA and Raman terms. Note that 2PA turns on when the sum of the frequencies is equal to the bandgap, but the Raman term turns on when the difference of the frequencies is equal to the bandgap so that one frequency must exceed the bandgap.

C. Linear and Quadratic Stark Effects

In addition to multiphoton absorption processes which involve the absorption or emission of a photon from both light fields, there can be a change in the absorption coefficient due to a shift in bandgap as a result of the ac Stark effect. For example, a change in the linear absorption of ω_1 occurs when the bands are shifted due to the ac Stark effect caused by ω_2. Two terms arise out of this as the $\boldsymbol{A} \cdot \boldsymbol{p}$ radiation perturbation term couples 1) the conduction (or valence) band to itself, which we will term the linear Stark effect (LSE), and 2) the conduction band to the valence band, which we will term the quadratic Stark effect (QSE). In a physical sense, the effect of the LSE on the linear absorption is essentially a reduction of the oscillator strength by renormalizing the interband coupling due to the acceleration of the electrons (or holes) in their final dressed state. The QSE, on the other hand, alters the linear absorption through blue shifting the bandgap.

The linear Stark shift (self-coupling) can be obtained from the previous calculation by expanding the zero-order Bessel function to the next higher order term in (20), $J_0(x) \simeq 1 - x^2/4$. This results in a modification to the S-matrix term which describes the one-photon absorption. The transition rate for the single-photon absorption of ω_1 is then modified as

$$W = \sum_{\text{spin}} \int \frac{d^3k}{(2\pi)^3} \left[\frac{\pi e A_{01}}{m_0 c}\right]^2 |\hat{a} \cdot \boldsymbol{p}_{vc}|^2 \cdot \left[1 - \left(\frac{eA_{02}}{2m_{vc} c\omega_2}\right)^2 |\boldsymbol{k} \cdot \hat{a}|^2\right]^2 \cdot \frac{1}{2\pi\hbar} \delta\left(E_g + \frac{\hbar^2 k^2}{2m_{vc}} - \hbar\omega_1\right). \tag{31}$$

On performing this integral over k space and considering the term proportional to $I_1 I_2$, the following is obtained for the change in the transition rate:

$$\Delta W = -\frac{2^5\pi}{5} \frac{e^4}{n_1 n_2 c^2} \frac{m_c^{1/2} |\boldsymbol{p}_{vc}|^2}{m_0^2} \frac{I_1 I_2}{(\hbar\omega_1)^2 (\hbar\omega_2)^4} \cdot (\hbar\omega_1 - E_g)^{3/2}. \tag{32}$$

The resultant change of absorption $\Delta\alpha$ can be given in terms of (28) with F_2 given by

$$F_2^{\mathrm{LSE}}(x_1; x_2) = -\frac{(x_1 - 1)^{3/2}}{2^6 x_1 x_2^4} \tag{33}$$

where the scaling is the same as in (28).

The quadratic Stark shift resulting from the coupling between the conduction and valence bands due to ω_2 is given by

$$\Delta E_{cv} = -\Delta E_{vc} = \left(\frac{eA_{02}}{2m_0 c}\right)^2 |\hat{a} \cdot \boldsymbol{p}_{vc}|^2 \left[\left(E_g + \frac{\hbar^2 k^2}{2m_{vc}} - \hbar\omega_2\right)^{-1} + \left(E_g + \frac{\hbar^2 k^2}{2m_{vc}} + \hbar\omega_2\right)^{-1}\right]. \tag{34}$$

It should be expected that in the low-frequency limit $\hbar\omega_2 \ll E_g$, the energy shift due to the QSE as given by the above equations would approach the classical pondermotive energy of the electron/hole in an oscillating electromagnetic field. This equivalence can indeed be simply verified by substituting $|\boldsymbol{p}_{vc}|$ from (23) into (34), which would yield

$$\Delta E_e = -\Delta E_h = \frac{e^2 A_{02}^2}{4m_c c^2}. \tag{35}$$

This classical energy shift, which is also referred to as the "mass energy shift," has been used in previous "dressed state" (tunneling) calculations of the interband transition rate [28], [30].

Returning to the QSE energy shift, we note that this energy term is time independent (i.e., nonoscillating). Therefore, it only appears in the δ-function energy conservation terms. Thus, the one-photon transition rate is modified to give

$$W = \sum_{\text{spin}} \int \frac{d^3k}{(2\pi)^3} \left[\frac{\pi e A_{01}}{m_0 c}\right]^2 |\hat{a} \cdot \boldsymbol{p}_{vc}|^2 \frac{1}{2\pi\hbar} \cdot \delta\left(E_g + \frac{\hbar^2 k^2}{2m_{vc}} + \Delta E_{cv} - \Delta E_{vc} - \hbar\omega_1\right). \tag{36}$$

On performing the integration and expanding to obtain the term proportional to $I_1 I_2$, the change in the transition rate is given as

$$\Delta W = -\frac{4\pi}{5} \frac{e^4}{n_1 n_2 c^2} \frac{m_c^{3/2} |\boldsymbol{p}_{vc}|^4}{m_0^4} \frac{I_1 I_2}{(\hbar\omega_1)^2 (\hbar\omega_2)^2} \cdot (\hbar\omega_1 - E_g)^{-1/2} \left[\frac{1}{\hbar\omega_1 - \hbar\omega_2} + \frac{1}{\hbar\omega_1 + \hbar\omega_2}\right]. \tag{37}$$

TABLE I
FREQUENCY DEPENDENCE OF THE NONDEGENERATE ABSORPTION $F_2(\hbar\omega_1/E_g; \hbar\omega_2/E_g)$ AS DEFINED IN (28)

Contribution	$F_2(x_1; x_2)$
Two-Photon Absorption	$\frac{(x_1 + x_2 - 1)^{3/2}}{2^7 x_1 x_2^2}\left(\frac{1}{x_1} + \frac{1}{x_2}\right)^2$
Raman	$\frac{(x_1 - x_2 - 1)^{3/2}}{2^7 x_1 x_2^2}\left(\frac{1}{x_1} - \frac{1}{x_2}\right)^2$
Linear Stark	$-\frac{(x_1 - 1)^{3/2}}{2^6 x_1 x_2^2}\frac{1}{x_2^2}$
Quadratic Stark	$-\frac{1}{2^{10} x_1 x_2^2 (x_1 - 1)^{1/2}}\left[\frac{1}{x_1 - x_2} + \frac{1}{x_1 + x_2}\right]$

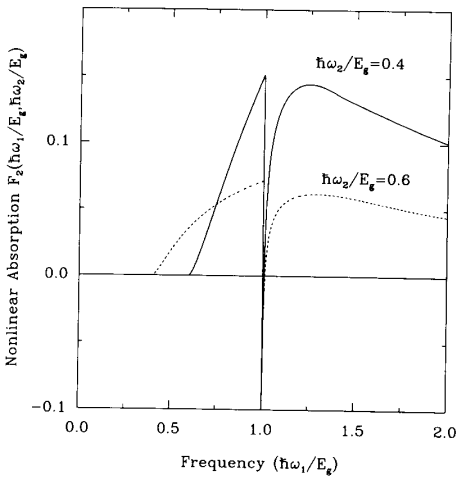

Fig. 3. Theoretical frequency dependence of the nondegenerate nonlinear absorption for two different "pump" frequencies $\hbar\omega_2/E_g = 0.4, 0.6$. Below the fundamental absorption edge $\hbar\omega_1 < E_g$, only 2PA contributes to the nonlinear absorption.

The resulting change in absorption coefficient is given by (28) with

$$F_2^{\mathrm{QSE}}(x_1; x_2) = -\frac{1}{2^{10} x_1 x_2^2 (x_1 - 1)^{1/2}}\left[\frac{1}{x_1 - x_2} + \frac{1}{x_1 + x_2}\right] \tag{38}$$

Again, the total $\Delta\alpha(\omega_1; \omega_2)$ is given by (28) and using the sum of all the F_2 terms for multiphoton and Stark shift terms. These results for the spectrum of the nondegenerate absorption change for the two-band model with parallel optical polarization vectors and $\hbar\omega_2 < E_g$ are summarized in Table I.

The spectrum of the nonlinear absorption $F_2(\hbar\omega_1/E_g; \hbar\omega_2/E_g)$ is shown in Fig. 3 for two different "pump" frequencies ω_2. Note that for $\hbar\omega_2 < E_g$, the Raman and Stark terms can only contribute to the nonlinear absorption for $\hbar\omega_1 > E_g$. The negative (i.e., decreasing absorption) divergence at the bandgap results from the quadratic Stark shift causing a blue shift of the band edge. The spectrum in Fig. 3 resembles that obtained by Yacoby [36], who calculated the interband transition rate when the modulating source (ω_2) is of very low frequency (i.e., RF excitation) and the resonant ac Stark effect is neglected.

IV. NONLINEAR REFRACTION

In general, we can evaluate the nondegenerate refractive index change $\Delta n(\omega; \Omega)$ as given by the Kramers–Krönig dispersion relation:

$$\Delta n(\omega; \Omega) = \frac{c}{\pi}\int_0^\infty \frac{\Delta\alpha(\omega'; \Omega)}{\omega'^2 - \omega^2}\, d\omega'. \tag{39}$$

However, there are few experiments which measure this quantity other than at $\Omega = \omega$. We therefore present in this paper only the calculated results for the degenerate $\Delta n(\omega; \omega)$ which, in turn, will lead to the Kerr coefficients n_2 or γ as defined by (1):

$$\gamma = K\frac{\hbar c\sqrt{E_p}}{n_0^2 E_g^4} G_2\left(\frac{\hbar\omega}{E_g}\right) \tag{40}$$

where the dispersion function G_2 is given by

$$G_2(x_2) = \frac{2}{\pi}\int_0^\infty \frac{F_2(x_1; x_2)\, dx_1}{x_1^2 - x_2^2}. \tag{41}$$

We have neglected any dispersion in the linear refractive index n_0 in the integral. The magnitude of the dispersion is typically only 10% of the background refractive index around the band edge of semiconductors, so we do not anticipate any significant error. All that remains is for the above integral to be evaluated for the various contributions to the nondegenerate absorption $F_2(x_1; x_2)$. All of the integrals are performed in a similar manner and make use of the identity

$$\int_0^\infty \frac{x^{\mu-1}\, dx}{(a + x)^n} = a^{\mu-n}\frac{\Gamma(\mu)\Gamma(n - \mu)}{\Gamma(n)} \tag{42}$$

for $n > \mu$. The individual contributions are given in Table II.

On examining the low-frequency limit, it is found that these terms diverge as $\omega \to 0$. In order to investigate such unphysical "infrared" divergences, we go one step back and examine the nondegenerate case as given by (39). This equation indicates that, in general, $\Delta n(\omega; \Omega)$ is not divergent in ω, and therefore any zero-frequency divergence must be in the pump frequency Ω as it appears in $\Delta\alpha$. To

TABLE II
DISPERSION OF THE NONLINEAR REFRACTION $G_2(\hbar\omega/E_g)$ FOR FREQUENCIES BELOW THE BAND EDGE AS DEFINED IN (44). $\Theta(x)$ IS THE HEAVISIDE OR STEP FUNCTION.

Contribution	$G_2(x)$
Two-Photon Absorption	$\frac{1}{(2x)^6}\left[-\frac{3}{8}x^2(1-x)^{-1/2}+3x(1-x)^{1/2}-2(1-x)^{3/2}+2\Theta(1-2x)(1-2x)^{3/2}\right]$
Raman	$\frac{1}{(2x)^6}\left[-\frac{3}{8}x^2(1+x)^{-1/2}-3x(1+x)^{1/2}-2(1+x)^{3/2}+2(1+2x)^{3/2}\right]$
Linear Stark	$\frac{1}{(2x)^6}[2-(1-x)^{3/2}-(1+x)^{3/2}]$
Quadratic Stark	$\frac{1}{2^{10}x^5}\left[(1-x)^{-1/2}-(1+x)^{-1/2}-\frac{x}{2}(1-x)^{-3/2}-\frac{x}{2}(1+x)^{-3/2}\right]$
Divergent Term	$\frac{1}{(2x)^6}\left[-2-\frac{35x^2}{8}+\frac{x}{8}(3x-1)(1-x)^{-1/2}-3x(1-x)^{1/2}+(1-x)^{3/2}+\frac{x}{8}(3x+1)(1+x)^{-1/2}+3x(1+x)^{1/2}+(1+x)^{3/2}\right]$

further identify these divergences, $\Delta n(\omega; \Omega)$ can be expanded as a Laurent series around $\Omega = 0$. We find that there exist terms which diverge as Ω^{-4}, Ω^{-3}, Ω^{-2}, and Ω^{-1}. On summing these terms, however, all the divergences vanish apart from a term proportional to Ω^{-2}, leaving the divergent term as

$$G_2^{\text{div}} = \frac{g(\omega)}{\Omega^2} \tag{43}$$

where $g(\omega)$ has no divergence at $\omega = 0$. Now, by setting $\Omega = \omega$, one arrives at the degenerate divergence function as shown in Table II. This diverging term is expected as $\boldsymbol{A} \cdot \boldsymbol{p}$ perturbation theory has been used in the transition rate calculations, and it is well known that divergences of this order can be introduced [37], whereas the comparable $\boldsymbol{E} \cdot \boldsymbol{r}$ perturbation theory avoids such divergences. The latter perturbation technique, however, is not suitable for solids with extended wavefunctions, and simple scaling rules cannot be easily derived. In a similar manner to Moss *et al.* [38], we treat such a divergence as unphysical and subtract it from the result for the nonlinear refraction.

The individual contributions to the nonlinear refraction are shown in Fig. 4 as a function of frequency. The divergence in each physically identifiable process has been subtracted for clarity. It can be seen that the most significant contribution to the spectral dependence of G_2 arises from the 2PA term, except close to the band edge where the quadratic Stark term becomes dominant. The linear Stark term arising from the self-coupling of the bands is insignificant compared to the quadratic term. In terms of second-order perturbation theory, this is a result of the momentum matrix element being much larger when taken between conduction and valence bands than between the same bands [13]. The only significance of the linear Stark term in the present calculation is that it cancels terms which diverge as ω^{-4} arising from the 2PA and Raman contributions.

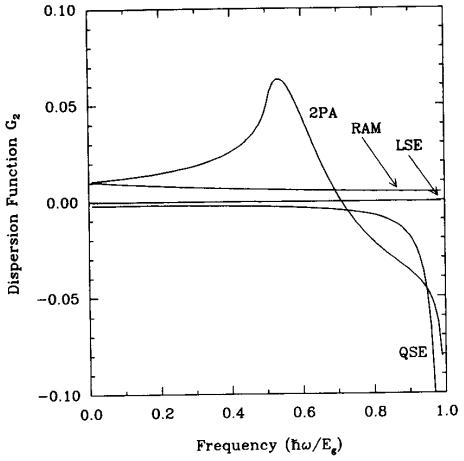

Fig. 4. Frequency dependence of the various contributions to the nonlinear refractive index n_2. Each contribution is derived from a Kramers–Krönig transform of the various nonlinear absorption processes: two-photon absorption, Raman transitions, and linear and quadratic Stark shifts of the band edge. The divergence of each term as $\omega \to 0$ has been removed for clarity.

The general scaled form for n_2 is given by

$$n_2 \text{ (esu)} = K' \frac{\sqrt{E_p}}{n_0 E_g^4} G_2(\hbar\omega/E_g) \tag{44}$$

where, using the value of K obtained from the fit to 2PA in semiconductors (3100), the constant $K' = 1.50 \times 10^{-8}$ when E_g and E_p are defined in eV. Using the value of K predicted by theory (no fitting) gives $K' = 0.94 \times 10^{-8}$. We note the E_g^{-4} dependence for the magnitude of n_2, corresponding to the scaling predicted by Wherrett [13].

A graphical comparison of the dispersion function $G_2(\hbar\omega/E_g)$ with measured values of n_2 is shown in Fig. 5(a). The values for semiconductors (squares) were obtained from Z-scan measurements at 1.06 and 0.53 μm [1], [10] (as previously plotted in Fig. 1). Included in these data are some new measurements. We also show "nearly degenerate three-wave mixing" n_2 measurements of large-gap optical materials [6] (solid circles) and a measurement of n_2 in silica at 249 nm [39] (diamond).

Fig. 5(b) shows the extension to Fig. 5(a) for frequencies close to the band edge where the bound electronic refractive nonlinearity shows a resonance due to the quadratic ac Stark effect. This graph also includes recent measurements of n_2 in AlGaAs by LaGasse *et al.* [40] using femtosecond time-division interferometry techniques (solid triangles). Table III shows the measured values for n_2 for the various semiconductors and wide-gap optical solids which are plotted in Fig. 5. The data for the semiconductor bandgaps and linear refractive index were obtained from [41], [42]. From the theory presented here, we also give the predicted values for n_2. For the semiconductor measurements at 1.06 and 0.53 μm (excluding CdSe at 1.06 μm whose n_2 could not be measured with any degree of accuracy because of the 2PA-induced band-filling refractive nonlinearity), we find an average difference of less than 30% between the measured and predicted values. Including the measurements for dielectrics, the average difference was less than a factor of 2. We note, however, that the measured n_2 for these wide-gap solids are consistently smaller than the predicted values. One possible reason for this is that the absorption edge has been used to determine the bandgap. The band structure for these materials is not well known, and the direct gap may well be larger than this. We find, however, for these wide-gap materials, that a good fit to the n_2 data can be obtained by using a smaller value for the constant K' $= 0.86 \times 10^{-8}$, as shown by the dashed line in Fig. 5(a).

For frequencies close to the band edge, the Stark effect results in a divergence in the nonlinear refractive index of $-(E_g - \hbar\omega)^{-3/2}$. This region can be examined in more detail by replotting data and theory in a log-log plot as shown in Fig. 6. Note the straight line dependence for small detunings, with a slope of $-3/2$ corresponding to the above asymptotic relationship. From Figs. 5(b) and 6, one notices an increasing deviation of the AlGaAs data from the theory as the photon energy is approaching the energy gap. One possible cause for this deviation is the excitonic enhancement which becomes significant near the band edge.

The Stark effect can also be described as virtual band blocking since a blue shift of the band edge is equivalent

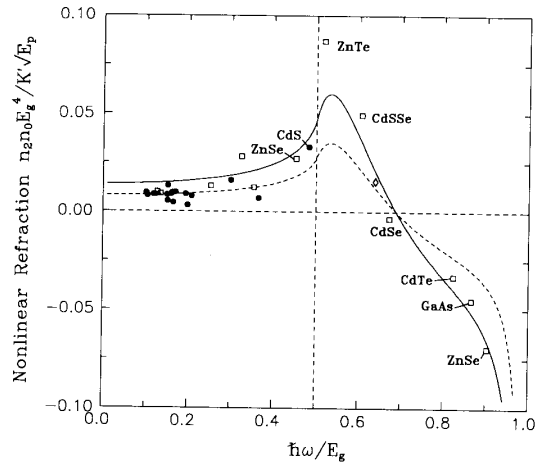

(a)

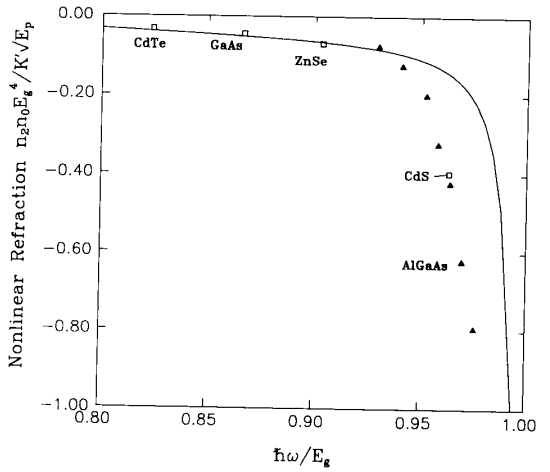

(b)

Fig. 5. (a) Dispersion of the nonlinear refractive index n_2. Data for n_2 are scaled as $n_2 n_0 E_g^4/K'\sqrt{E_p}$. The circles are measurements in [6], the diamond is from [39], and the squares are our own Z-scan measurements. We have labeled the semiconductor data. The solid line is the $G_2(\hbar\omega/E_g)$ function derived here for a two-band model of a semiconductor using the 2PA data for the fit to the constant K'. The dashed line corresponds to a fit to n_2 for the wide-gap solids ($K' = 0.86 \times 10^{-8}$). (b) Extension of (a) to frequencies close to the band edge. The triangles are n_2 measurements of AlGaAs in [40].

to a reduction of optically coupled states at photon energies corresponding to the bottom of the band (in a similar manner to the dynamic Burstein–Moss shift [43]). Indeed, the direct saturation model [44] predicts exactly the same frequency and material dependence of the nonlinear refractive index just beneath the band edge. This allows a conceptual link between below-gap (virtual carriers) and bandgap resonant (real carriers) nonlinear optical effects [45].

Hidden in Figs. 5 and 6 is the E_g^{-4} scaling of n_2 that gives a variation of n_2 from 2.5×10^{-14} esu for a material

TABLE III

LIST OF n_2 DATA SHOWING PARAMETERS USED IN THE CALCULATION (FROM [41], [42]) ALONG WITH THE EXPERIMENTALLY MEASURED AND THEORETICALLY PREDICTED VALUES OF n_2. THESE n_2 DATA INCLUDE MEASUREMENTS IN [6], [39], [40]. † INDICATES WHERE WE HAVE USED THE DIRECT GAP RATHER THAN THE FUNDAMENTAL ABSORPTION EDGE. THE COLUMN INDICATED BY * USES A FIT TO THE CONSTANT K' FOR WIDE-GAP MATERIALS RATHER THAN THE FIT TO 2PA IN SEMICONDUCTORS [SEE FIG. 5(a)]

Material	Wavelength (μm)	Bandgap (eV)	Refr. Index	n_2 (Exp.) $\times 10^{-13}$ (esu)	n_2 (Pred.) $\times 10^{-13}$ (esu)	n_2 (Pred.)* $\times 10^{-13}$ (esu)
Ge	10.6	0.87†	4.00	2700	4400	
GaAs	1.06	1.35	3.47	−2700	−3100	
CdTe	1.06	1.44	2.84	−2000	−2100	
CdSe	1.06	1.74	2.56	−90	180	
$CdS_{0.5}Se_{0.5}$	1.06	1.93	2.45	1000	720	
ZnTe	1.06	2.26	2.79	830	540	
CdS	0.53	2.42	2.34	−3400	−1200	
ZnSe	1.06	2.58	2.48	170	190	
ZnSe	0.53	2.58	2.70	−400	−380	
SBN	1.06	3.3	2.4	30	51	29
ZnS	1.06	3.54	2.40	48	36	
KTP	1.06	3.54	1.78	13	49	28
BaF_2	1.06	9.21	1.47	0.67	0.95	0.54
BaF_2	0.53	9.21	1.47	0.85	1.10	0.63
AlGaAs	0.850	1.57	3.30	−2000	−2800	
AlGaAs	0.840	1.57	3.30	−4000	−3300	
AlGaAs	0.830	1.57	3.30	−7000	−3900	
AlGaAs	0.825	1.57	3.30	−10000	−4300	
AlGaAs	0.820	1.57	3.30	−14000	−4900	
AlGaAs	0.815	1.57	3.30	−20000	−5900	
AlGaAs	0.810	1.57	3.30	−26000	−7300	
CdS	1.06	2.42	2.34	280	330	
AgCl	1.06	3.10	2.07	23	81	46
ZnO	1.06	3.20	1.96	23	73	41
NaBr	1.06	5.63	1.64	3.3	6.6	3.8
$CaCo_3$	1.06	5.88	1.60	1.1	5.6	3.2
KBr	1.06	6.04	1.56	2.9	5.1	2.9
KCl	1.06	6.89	1.49	2.0	3.1	1.8
KDP	1.06	6.95	1.60	0.7	2.8	1.6
KH_2PO_4	1.06	7.12	1.50	0.8	2.7	1.5
NaCl	1.06	7.21	1.53	1.6	2.5	1.4
Al_2O_3	1.06	7.30	1.75	1.2	2.1	1.2
KF	1.06	7.75	1.36	0.75	2.1	1.2
MgO	1.06	7.77	1.70	1.6	1.6	0.94
SiO_2	1.06	7.80	1.40	1.1	2.0	1.1
SrF_2	1.06	9.54	1.44	0.50	0.84	0.48
CaF_2	1.06	9.92	1.43	0.43	0.72	0.41
MgF_2	1.06	11.27	1.38	0.25	0.44	0.25
LiF	1.06	11.60	1.39	0.26	0.39	0.22
SiO_2	0.249	7.80	1.60	1.7	2.4	1.4

such as MgF_2 at 1.06 μm to -2.6×10^{-9} esu for AlGaAs at 810 nm [40] and 2.7×10^{-10} esu for Ge at 10.6 μm, which we measured with a picosecond CO_2 laser. This five orders of magnitude variation of n_2 is better displayed by plotting n_2 scaled by n_0 and G_2 as a function of E_g on a log–log plot, as shown in Fig. 7. In spite of this very large variation in the magnitude of n_2 (and the change in sign), this extremely simple model gives good agreement with the data for materials including both semiconductors and insulators. It is found that the E_g^{-4} scaling law holds true over the five orders of magnitude variation in the modulus of n_2 for the data presented here. Additionally note that although the measured values of n_2 for ZnSe at 1.06 and 0.53 μm have different signs, both measurements are consistent with the scaling law.

V. IMPLICATIONS FOR ALL-OPTICAL SWITCHING

One of the applications of the nonlinear refractive index n_2 is in the role of all-optical switching. Some examples are a nonlinear Fabry–Perot filter for image processing, or parallel optical computing [46], [47], or coupled waveguides for communication switching networks [48], [7]. When it comes to optimizing devices for optical switching, it is important that optical losses in the system are not too large. For instance, if optical absorption is too large, then the change in refractive index will fall off rapidly as the optical beam propagates.

It can be shown that for any optical switching system, one must achieve a refractive index change Δn such that

$$|\Delta n| > c_{sw}\alpha\lambda \tag{45}$$

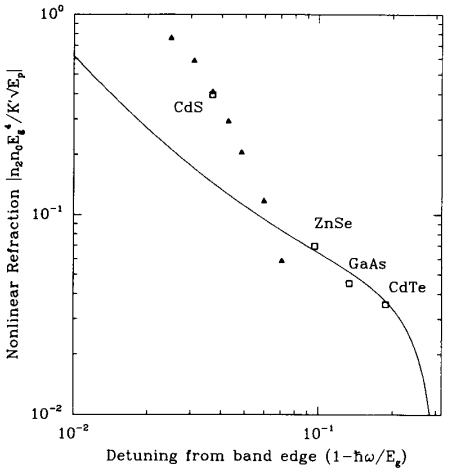

Fig. 6. Same as n_2 data close to the band edge as plotted in Fig. 5(b), but now plotted on a log-log scale to emphasize the asymptotic form $n_2 \propto -(1 - \hbar\omega/E_g)^{-3/2}$ as the frequency approaches the band edge. Again, the solid line shows the predicted form.

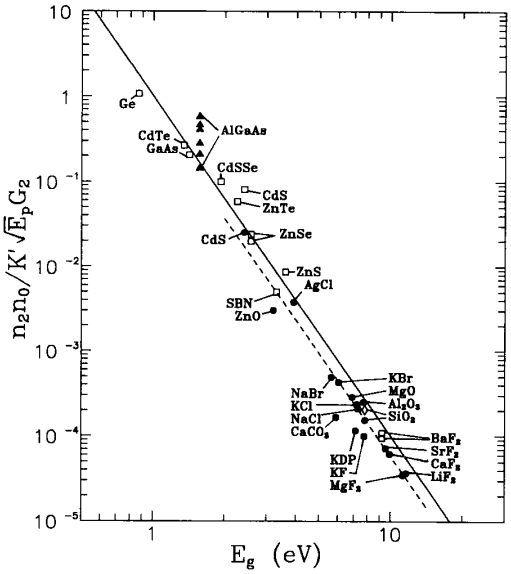

Fig. 7. A log-log plot showing the expected E_g^{-4} dependence of n_2. The data points are identical to those in Figs. 5 and 6, but now are scaled by the dispersion function $G_2(\hbar\omega/E_g)$. The solid line is the function E_g^{-4} which translates into a straight line of slope -4 on a log-log plot. The dashed line indicates the fit to the wide-gap solids which also have the E_g^{-4} dependence.

where c_{sw} is a numeric constant of the order of unity whose precise value depends on the exact switching scheme. For example, using a Fabry-Perot filter, $c_{sw} = (2\sqrt{3}\pi)^{-1}$ [49], whereas a nonlinear coupled waveguide gives $c_{sw} = 2$ [50], [51].

Below the band edge, the principal contribution to the absorption at irradiance levels of interest is two-photon absorption, $\alpha \simeq \beta I$. In addition, the electronic Kerr effect gives the change in refractive index $\Delta n = \gamma I$. Hence, in this regime, the requirement for all-optical switching is [50]

$$\left|\frac{\gamma}{\beta\lambda}\right| > c_{sw}. \tag{46}$$

The theory presented in this paper gives the scaling and dispersion for both β and γ, which are related through nonlinear Kramers-Krönig relations. Inserting the functional forms of β and γ given here gives the frequency dependence for the all-optical switching requirement:

$$\frac{\hbar\omega}{E_g}\frac{|G_2(\hbar\omega/E_g)|}{F_2(\hbar\omega/E_g)} > 2\pi c_{sw}. \tag{47}$$

Note that (47) has no explicit material dependence since it is only a function of the ratio $\hbar\omega/E_g$. Thus, although n_2 can be enhanced by using smaller gap materials, this does not necessarily improve the conditions for switching. The left-hand side of (47) is plotted in Fig. 8. In the same figure, we also show the experimentally measured values for this parameter $|2\pi\gamma/\beta\lambda|$ for some semiconductors using the n_2 values measured here and our 2PA coefficients from [11]. We note that there is a range of optical frequencies where this quantity becomes too small for optical switching, which is given approximately by $0.6 < \hbar\omega/E_g < 0.9$. This region is centered around the point where there is a change of sign in n_2, covering most of the range of frequencies where 2PA is observed. Therefore, given a certain wavelength of operation, this immediately excludes certain materials from consideration for all-optical switching. This was first noted by Stegeman *et al.* [50]. DeLong and Stegeman [52] recently used the results of [2], which only included the 2PA contribution to γ, to give a similar requirement for all-optical

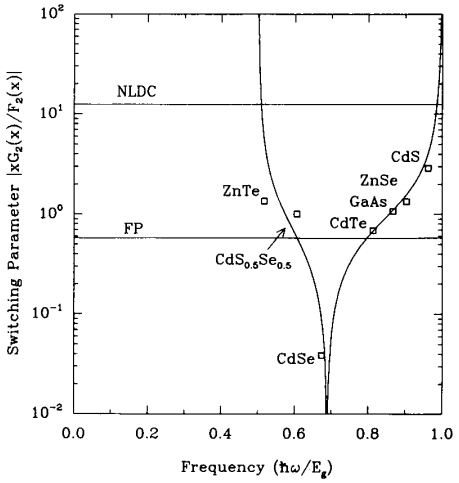

Fig. 8. Material-independent switching parameter as a function of frequency. Also shown are the minimum limits for all-optical switching in two different geometries: nonlinear directional coupler (NLDC) and Fabry-Perot (FP) filter. For switching to be possible, the switching parameter must exceed the relevant limit. The experimentally determined values of this parameter are based on the semiconductor n_2 measurements here and our β measurements in [11].

switching. Our result ignores free-carrier absorption and refraction, exciton effects, and linear absorption which may further restrict or enhance the choice of material.

This result can also be extended to other applications for nonlinear optics. For instance, 2PA has been a problem in the observation of spatial optical solitons based on the electronic Kerr effect [53]. We can use the above result as a rule of thumb in determining for what material/frequency combination 2PA would cause problems for nonlinear refractive applications.

VI. Conclusions

We have presented a simple two-band model calculation that gives a universal bandgap scaling and dispersion of the electronic Kerr effect in solids. This simple model, for the first time, draws a direct relationship between the nonlinear refractive index n_2 and its nonlinear absorptive counterparts, namely, two-photon absorption, Raman transitions, and the ac Stark effect. We have also presented measurements of the bound electronic nonlinear refractive index for various materials beneath the band edge. Several new data, along with previously published data, are compared to this theory, and remarkable agreement is observed.

A wide range of theoretical papers exists where nonlinear absorption is calculated by means of transition rates. We used a nonlinear Kramers–Krönig transformation approach to obtain the nonlinear refraction in terms of this electronic nonlinear absorption because this method circumvents a direct calculation of the complex nonlinear susceptibility. However, it is necessary to know the nondegenerate absorption in order to perform the calculation (or refraction in the equivalent converse expression). That is, we need expressions for the nonlinear absorption at all frequencies ω_1 when an optical field ω_2 is applied. This can be thought of as a pump–probe spectrum where, in the present convention, ω_2 would be the pump frequency and ω_1 the variable probe frequency. We calculated this nondegenerate nonlinear absorption using a simple two-band model for a direct gap semiconductor. The next stage of complexity would be to do the same calculation for the Kane four-band model of a semiconductor. It was necessary to include transitions over all frequencies so that the Raman and Stark shift terms are included, as well as two-photon absorption.

We performed the Kramers–Krönig integral on the nondegenerate nonlinear absorption to obtain analytic expressions for the nonlinear self-refraction. In this calculation, we set the two frequencies in the nonlinear refraction equal to determine self-refraction, but in general the nondegenerate refraction can also be obtained, i.e., the change in refractive index seen by the light of frequency ω when the light of frequency Ω is present.

Comparing the experimentally measured values of n_2 to the theoretical dispersion presented here, we find that good agreement is obtained over a wide range of frequencies and materials, with only one fitting paramter K' obtained from 2PA measurements in semiconductors. We note, however, that the theoretical value for this parameter is only about 40% smaller than this fitted value for K'. This is quite remarkable, and to some extent surprising as a simple two-band model has been used to calculate the nonlinear refraction with no account for the full-band structure or excitonic effects. However, as has been shown by earlier calculations of the 2PA coefficients in semiconductors [15], the effect of nonparabolicity of the bands becomes important only for small-gap semiconductors such as InSb. Also ignored in this model is the contribution of higher bands (conduction or split-off valence bands), and hence the effect of their specific structure. This can be justified by noticing the strong inverse photon energy dependence of the nonlinear transition rate as shown in Table I. This is better illustrated in Fig. 3 where the change in absorption becomes progressively smaller at higher frequencies ($\hbar\omega/E_g > 1.5$), and hence the near-gap transitions will dominate. Including the effect of higher bands in calculating the transition rate will contain terms involving high-energy photons, and therefore, it should have a negligible effect.

The other important simplification in our model has been the exclusion of the coulomb interaction or excitonic enhancement. Earlier calculations of the excitonic effects on two-photon transition rates had indicated a significant enhancement near the two-photon resonance $\hbar\omega \approx E_g/2$ [15], [21]. For example, the underestimation of both n_2 and the 2PA coefficient β of ZnTe at $\lambda = 1.06$ μm may well be due to this two-photon exciton resonance [11]. Similarly, for photon energies approaching the energy gap, an excitonic enhancement of the quadratic Stark effect is expected. For example, nonlinear refraction can occur due to the ac Stark shift of an exciton resonance [54]. We also expect the contribution from the quadratic Stark effect to be relatively larger when a four-band model for a semiconductor is used since the density of the valence band states is larger, which also may lead to a better fit. Therefore, the deviation of the measured n_2 data on CdS (at 532 nm) and AlGaAs (at $\sim$800 nm) from the predicted values may be due to these other near-bandgap effects.

It is also remarkable that the theory gives a reasonable fit to the data for large-gap optical materials, as well as conventional semiconductors. However, it can be seen that the predicted value for n_2 is consistently on the large side for these materials. This may be due to the fact that the absorption edge has been used to determine the direct bandgap. We find that for Ge, as expected, it is necessary to use the direct bandgap rather than the smaller indirect gap in order to obtain a satisfactory fit, and the same should be true for wide-gap solids. This is because the transitions involving the lower indirect gaps require phonon scattering, and thus they should have a smaller oscillator strength than direct interband transitions. Unfortunately, the band structure of these materials is not well known. We have also used the mean value of E_p for

semiconductors in order to predict n_2, and this parameter may also be quite different in other materials. We find that for the wide-gap solid data presented here, a better estimate for n_2 is obtained by replacing the K' from the fit to the semiconductor 2PA data with a smaller value, which may be more appropriate for these wide-gap materials, as indicated in Fig. 5(a) and Table III.

The change in sign of n_2 at about $\hbar\omega/E_g \simeq 0.7$ is predicted and observed. It is also demonstrated that the expected E_g^{-4} bandgap dependence holds true for a five order of magnitude variation in the modulus of n_2.

It is noted that the main contribution to the dispersion of n_2 below the bandgap arises from the two-photon transition term, with the Stark shift term becoming dominant close to the band edge. This partly explains the good fit obtained by using the quasi-nondegenerate two-photon absorption alone, as shown in a previous letter by the authors [2]

Acknowledgment

The authors thank A. Miller, O. Heinonen, S. Epifanov, and B. S. Wherrett for useful discussions, and A. Said, T. Wei, E. Canto, and J. Young for taking and analyzing portions of the n_2 data.

References

[1] M. Sheik-Bahae, A. A. Said, T. H. Wei, D. J. Hagan, and E. W. Van Stryland, "Sensitive measurements of optical nonlinearities using a single beam," *IEEE J. Quantum Electron.*, vol. 26, pp. 760-769, 1990.

[2] M. Sheik-Bahae, D. J. Hagan, and E. W. Van Stryland, "Dispersion and band-gap scaling of the electronic Kerr effect in solids associated with two-photon absorption," *Phys. Rev. Lett.*, vol. 65, pp. 96-99, 1990.

[3] D. J. Hagan, E. Canto, E. Meisak, M. J. Soileau, and E. W. Van Stryland, "Picosecond degenerate four-wave mixing studies in ZnSe," in *Tech. Dig. Conf. Lasers Electro-Opt.*, Anaheim, CA, 1988, vol. 7, p. 160.

[4] D. H. Auston *et al.*, "Research on nonlinear optical materials: An assessment," *Appl. Opt.*, vol. 26, pp. 211-234, 1987.

[5] D. A. B. Miller, M. H. Mozolowski, A. Miller, and S. D. Smith, "Nonlinear optical effects in InSb with a c.w. CO laser," *Opt. Commun.*, vol. 27, pp. 133-136, 1978.

[6] R. Adair, L. L. Chase, and S. A. Payne, "Nonlinear refractive index of optical crystals," *Phys. Rev. B*, vol. 39, pp. 3337-3349, 1989.

[7] S. R. Friberg, A. M. Weiner, Y. Silberberg, B. G. Sfez, and P. S. Smith, "Femtosecond switching in a dual-core fibre nonlinear coupler," *Opt. Lett.*, vol. 13, pp. 904-906, 1988.

[8] M. J. Soileau, W. E. Williams, N. Mansour, and E. W. Van Stryland, "Laser-induced damage and the role of self-focusing," *Opt. Eng.*, vol. 28, pp. 1133-1144, 1989.

[9] E. W. Van Stryland, Y. Y. Wu, D. J. Hagan, M. J. Soileau, and K. Mansour, "Optical limiting with semiconductors," *J. Opt. Soc. Amer. B*, vol. 5, pp. 1980-1989, 1988.

[10] M. Sheik-Bahae, A. A. Said, and E. W. Van Stryland, "High sensitivity, single beam n_2 measurements," *Opt. Lett.*, vol. 14, pp. 955-957, 1989.

[11] E. W. Van Stryland, H. Vanherzeele, M. A. Woodall, M. J. Soileau, A. L. Smirl, S. Guha, and T. F. Boggess, "Two photon absorption, nonlinear refraction, and optical limiting in semiconductors," *Opt. Eng.*, vol. 24, pp. 613-623, 1985.

[12] E. J. Canto-Said, D. J. Hagan, J. Young, and E. W. Van Stryland, "Degenerate four-wave mixing measurements of high order nonlinearities in semiconductors," *IEEE J. Quantum Electron.*, to be published.

[13] B. S. Wherrett, "Scaling rules for multiphoton interband absorption in semiconductors," *J. Opt. Soc. Amer. B*, vol. 1, pp. 67-72, 1984.

[14] J. Callaway, *Quantum Theory of the Solid State.* New York: Academic, 1974, p. 540.

[15] M. H. Weiler, "Nonparabolicity and exciton effects in two-photon absorption in zincblende semiconductors," *Solid State Commun.*, vol. 39, pp. 937-940, 1981.

[16] S. S. Jha and N. Bloembergen, "Nonlinear optical susceptibilities in group-IV and III-V semiconductors," *Phys. Rev.*, vol. 171, pp. 891-898, 1968.

[17] C. Flytzanis, "Third-order optical susceptibilities in IV-IV and III-V semiconductors," *Phys. Lett.*, vol. 31A, pp. 273-274, 1970.

[18] J. A. Van Vechten and D. E. Aspnes, "Franz-Keldysh contributions to third-order optical susceptibilities," *Phys. Lett.*, vol. 30A, pp. 346-347, 1969.

[19] C. C. Wang, "Empirical relation between the linear and third-order nonlinear optical susceptibilities," *Phys. Rev. B*, vol. 2, pp. 2045-2048, 1970.

[20] N. L. Boling, A. J. Glass, and A. Owyoung, "Empirical relationships for predicting nonlinear refractive index changes in optical solids," *IEEE J. Quantum Electron.*, vol. QE-14, pp. 601-608, 1978.

[21] C. C. Lee and H. Y. Fan, "Two-photon absorption with exciton effect for degenerate bands," *Phys. Rev. B*, vol. 9, pp. 3502-3516, 1974.

[22] H. M. Nussenzveig, *Causality and Dispersion Relations.* New York: Academic, 1972.

[23] D. A. B. Miller, C. T. Seaton, M. E. Prise, and S. D. Smith, "Band-gap-resonant nonlinear refraction in III-V semiconductors," *Phys. Rev. Lett.*, vol. 47, pp. 197-200, 1981.

[24] B. S. Wherrett, D. Hutchings, and D. Russell, "Optically bistable interference filters: Optimization considerations," *J. Opt. Soc. Amer. B*, vol. 3, pp. 351-362, 1986.

[25] A. Yariv, *Quantum Electronics.* 2nd ed. New York: Wiley, 1975.

[26] S. M. Kogan, "On the electrodynamics of weakly nonlinear media," *Sov. Phys. JETP*, vol. 16, pp. 217-219, 1963.

[27] P. J. Price, "Theory of quadratic response functions," *Phys. Rev.*, vol. 130, pp. 1792-1797, 1963.

[28] L. V. Keldysh, "Ionization in the field of a strong electromagnetic wave," *Sov. Phys. JETP*, vol. 20, pp. 1307-1314, 1965.

[29] H. S. Brandi and C. B. de Araújo, "Multiphoton absorption coefficients in solids: A universal curve," *J. Phys. C: Solid State Phys.*, vol. 16, pp. 5929-5936, 1983.

[30] H. D. Jones and H. R. Reiss, "Intense-field effects in solids," *Phys. Rev. B*, vol. 16, pp. 2466-2473, 1977.

[31] D. M. Volkov, "Concerning a class of solutions of the Dirac equation," *Z. Phys.*, vol. 94, pp. 250-260, 1935.

[32] T.-Y. Wu and T. Ohmura, *Quantum Theory of Scattering.* Englewood Cliffs, NJ: Prentice-Hall, 1962.

[33] E. O. Kane, "Band structure of indium antimonide," *J. Phys. Chem. Solids*, vol. 1, pp. 249-261, 1957.

[34] P. Liu, W. L. Smith, H. Lotem, J. H. Bechtel, N. Bloembergen, and R. S. Adhav, "Absolute two-photon absorption coefficients at 355 and 266 nm," *Phys. Rev. B*, vol. 17, pp. 4620-4632, 1978.

[35] A. M. Johnson, C. R. Pidgeon, and J. Dempsey, "Frequency dependence of two-photon absorption in InSb and HgCdTe," *Phys. Rev. B*, vol. 22, pp. 825-831, 1980.

[36] Y. Yacoby, "High-frequency Franz-Keldysh effect," *Phys. Rev.*, vol. 169, pp. 610-619, 1968.

[37] J. M. Worlock, "Two-photon spectroscopy," in F. T. Arecchi and E. D. Schulz-DuBois, Ed., *Laser Handbook.* Amsterdam: North-Holland, 1972, pp. 1323-1369.

[38] D. J. Moss, E. Ghahramani, J. E. Sipe, and H. M. van Driel, "Band-structure calculation of dispersion and anisotropy in $\chi^{(3)}$ for third-harmonic generation in Si, Ge, and GaAs," *Phys. Rev. B*, vol. 41, pp. 1542-1560, 1990.

[39] I. N. Ross, W. T. Toner, C. J. Hooker, J. R. M. Barr, and I. Coffey, "Nonlinear properties of silica and air for picosecond ultraviolet pulses," *J. Modern Opt.*, vol. 37, pp. 555-573, 1990.

[40] M. J. LaGasse, K. K. Anderson, C. A. Wang, H. A. Haus, and J. G. Fujimoto, "Femtosecond measurements of the nonresonant nonlinear index in AlGaAs," *Appl. Phys. Lett.*, vol. 56, pp. 417-419, 1990.

[41] R. C. Weast, Ed., *CRC Handbook of Chemistry and Physics*, 65th ed. Boca Raton, FL: CRC Press, 1984.

[42] E. D. Palik, Ed., *Handbook of Optical Constants of Solids.* Orlando, FL: Academic, 1985.

[43] T. S. Moss, "Theory of intensity dependence of refractive index," *Phys. Status Solidi(b)*, vol. 101, pp. 555-561, 1980.

[44] B. S. Wherrett and N. A. Higgins, "Theory of nonlinear refraction near the band edge of a semiconductor," *Proc. Roy. Soc. London A*, vol. 379, pp. 67–90, 1982.
[45] B. S. Wherrett, "A comparison of theories of resonant nonlinear refraction in semiconductors," *Proc. Roy. Soc. London A*, vol. 390, pp. 373–396, 1983.
[46] B. S. Wherrett and S. D. Smith, "Bistable semiconductor elements for optical data processing and photonic logic," *Physica Scripta*, vol. T13, pp. 189–194, 1986.
[47] S. D. Smith, A. C. Walker, F. A. P. Tooley, and B. S. Wherrett, "The demonstration of restoring digital optical logic," *Nature*, vol. 325, pp. 27–31, 1987.
[48] P. LiKamWa, J. E. Stich, N. J. Mason, J. S. Roberts, and P. N. Robson, "All optical multiple-quantum-well waveguide switch," *Electron. Lett.*, vol. 21, pp. 26–27, 1985.
[49] D. C. Hutchings, C. H. Wang, and B. S. Wherrett, "Optically bistable interference filters: Self-consistent modeling of nonlinear optical characteristics and optimization," *J. Opt. Soc. Amer. B*, vol. 8, pp. 618–631, 1991.
[50] V. Mizrahi, K. W. DeLong, G. I. Stegeman, M. A. Saifi, and M. J. Andrejco, "Two-photon absorption as a limitation to all-optical switching," *Opt. Lett.*, vol. 14, pp. 1140–1142, 1989.
[51] K. W. DeLong, K. B. Rochford, and G. I. Stegeman, "Effect of two-photon absorption on all-optical guided-wave devices," *Appl. Phys. Lett.*, vol. 55, pp. 1823–1825, 1989.
[52] K. W. DeLong and G. I. Stegeman, "Two-photon absorption as a limitation to all-optical waveguide switching in semiconductors," *Appl. Phys. Lett.*, vol. 57, pp. 2063–2064, 1990.
[53] J. S. Aitchison, A. M. Weiner, Y. Silverberg, M. K. Oliver, J. L. Jackel, D. E. Leaird, E. M. Vogel, and P. W. E. Smith, "Observation of the fundamental spatial optical soliton in a glass waveguide," in *Proc. Opt. Soc. Amer. Annu. Meet.*, Orlando, FL, 1989, p. PD20.
[54] M. Lindberg and S. W. Koch, "Theory of the optical Stark effect in semiconductors under ultrashort-pulse excitation," *Phys. Status Solidi (b)*, vol. 150, pp. 379–385, 1988.

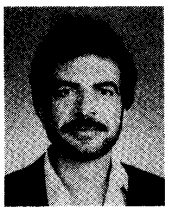

Mansoor Sheik-Bahae (M'87) was born in Isfahan, Iran, in 1956. He received the B.S. and M.S. degrees in electrical engineering from the Catholic University of America, Washington DC, in 1980 and 1982, respectively, and the Ph.D. degree in electrophysics from the State University of New York (SUNY) at Buffalo, in 1987.

He then joined the Center for Research in Electro-Optics and Lasers (CREOL) at the University of Central Florida, Orlando, where he is now an Assistant Research Professor in the area of nonlinear optics and ultrafast phenomena. His research activities have been concentrated on both the experimental and theoretical study of nonlinear optical processes in various materials, particularly in bulk semiconductors. He has also been involved in the development and characterization of the ultrafast (picosecond) CO_2 laser systems. He is currently investigating the ultrafast optical Kerr nonlinearities in semiconductors and organic materials with an emphasis on their applications to optical power limiting and all optical switching devices.

Dr. Sheik-Bahae is a member of the Optical Society of America.

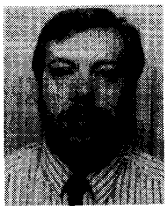

David Crichton Hutchings was born in Edinburgh, Scotland, on November 29, 1963. He received the B.Sc. degree and the Ph.D. degree on nonlinear refraction and optical bistability in semiconductors, from Heriot-Watt University, Edinburgh, in 1984 and 1988, respectively.

He was employed as a Research Associate at Heriot-Watt University from 1987 to 1990. He is currently employed as a Research Associate at the Center for Research in Electro-Optics and Lasers (CREOL), University of Central Florida, Orlando. His current research interests include nonlinear optics in semiconductors and carrier dynamics in quantum wells.

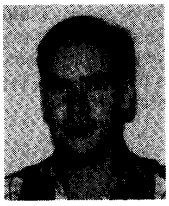

David J. Hagan (M'87) received the B.Sc. and Ph.D. degrees in physics in 1982 and 1985, respectively, from Heriot-Watt University, Edinburgh, Scotland. His Ph.D. dissertation was on the effects of carrier diffusion on resonant semiconductor nonlinear effects, such as phase conjugation, Sagnac-effect enhancement, and arrays of optically bistable switches. In 1982 and 1985, he worked as a student engineer in the Precision Instruments Group at Ferranti, plc. on reduction of scatter in ring laser gyroscopes.

From 1985 to 1987, he was a Research Scientist in the Center for Applied Quantum Electronics, North Texas State University, Denton, where he worked on optical nonlinearities and limiting in II–VI semiconductors. Currently, he is an Assistant Professor with the Department of Physics and the Center for Research in Electro-Optics and Lasers (CREOL) at the University of Central Florida, Orlando, where his current research interests are superconductive detectors and the fundamental mechanisms and applications of nonlinear optical processes in organic molecules, microcrystallites, and bulk semiconductors.

Eric W. Van Stryland (M'84–SM'90) was born in 1947. He received the Ph.D. degree in physics in 1976 from the University of Arizona, Tucson, where he worked at the Optical Sciences Center on optical coherent transients.

He worked in the areas of femtosecond pulse production, multiphoton absorption in solids, and laser-induced damage at the Center for Laser Studies at the University of Southern California, Los Angeles. He joined the Department of Physics at North Texas State University, Denton, in 1978 and was instrumental in forming the Center for Applied Quantum Electronics there. In 1987 he joined the newly formed Center for Research in Electro-Optics and Lasers (CREOL) at the University of Central Florida, Orlando, where he is a Professor with the Departments of Physics and Electrical Engineering, working in the area of nonlinear optics.